Differential neutralization and inhibition of SARS-CoV-2 variants by antibodies elicited by COVID-19 mRNA vaccines

Authors:

Li Wang[1]*, Markus H. Kainulainen[1]*, Nannan Jiang[1]*, Han Di[1]*, Gaston Bonenfant[1]*, Lisa Mills[1], Michael Currier[1], Punya Shrivastava-Ranjan[1], Brenda M. Calderon[1], Mili Sheth[1], Brian R. Mann[1], Jaber Hossain[1], Xudong Lin[1], Sandra Lester[1], Elizabeth Pusch[1], Joyce Jones[1], Dan Cui[1], Payel Chatterjee[1], Harley M. Jenks[1], Esther Morantz[1], Gloria Larson[1], Masato Hatta[1], Jennifer Harcourt[1], Azaibi Tamin[1], Yan Li[1], Ying Tao[1], Kun Zhao[1], Kristine Lacek[1], Ashely Burroughs[1], Terianne Wong[1], Suxiang Tong[1], John R. Barnes[1], Mark W. Tenforde[1], Wesley H. Self[2], Nathan I. Shapiro[3], Matthew C. Exline[4], D. Clark Files[5], Kevin W. Gibbs[5], David N. Hager[6], Manish Patel[1], Alison S. Laufer Halpin[1], Laura K. McMullan[1], Justin S. Lee[1], Xuping Xie[7], Pei-Yong Shi[7], C. Todd Davis[1], Christina F. Spiropoulou[1], Natalie J. Thornburg[1], M. Steven Oberste[1], Vivien Dugan[1], SSEV Bioinformatics Working Group, David E. Wentworth[1], Bin Zhou[1]

Affiliations:

[1]COVID-19 Emergency Response, Centers for Disease Control and Prevention, Atlanta, Georgia, USA

[2]Vanderbilt University, Nashville, Tennessee, USA

[3]Harvard University, Cambridge, Massachusetts, USA

[4]Ohio State University, Columbus, Ohio, USA

[5]Wake Forest Baptist Medical Center, Winston-Salem, North Carolina, USA

[6]Johns Hopkins University, Baltimore, Maryland, USA

[7]University of Texas Medical Branch, Galveston, Texas, USA

* These authors contributed equally to this study

Correspondence: dwentworth@cdc.gov; bzhou@cdc.gov

SSEV Bioinformatics Working Group: Dhwani Batra, Andrew Beck, Jason Caravas, Roxana Cintron-Moret, Peter W. Cook, Jonathan Gerhart, Christopher Gulvik, Norman Hassell, Dakota Howard, Kristen Knipe, Rebecca J. Kondor, Nicholas Kovacs, Kristine Lacek, Brian R. Mann, Laura K. McMullan, Kara Moser, Clinton R. Paden, Benjamin Rambo Martin, Matthew Schmerer, Samuel Shepard, Richard Stanton, Thomas Stark, Erisa Sula, Kendall Tymeckia, Yvette Unoarumhi

Introductory

The evolution of severe acute respiratory syndrome coronavirus 2 (SARS-CoV-2) has resulted in the emergence of many new variant lineages that have exacerbated the COVID-19 pandemic. Some of those variants were designated as variants of concern/interest (VOC/VOI) by national or international authorities based on many factors including their potential impact on vaccines. To ascertain and rank the risk of VOCs and VOIs, we analyzed their ability to escape from vaccine-induced antibodies. The variants showed differential reductions in neutralization and replication titers by post-vaccination sera. Although the Omicron variant showed the most escape from neutralization, sera collected after a third dose of vaccine (booster sera) retained moderate neutralizing activity against that variant. Therefore, vaccination remains the most effective strategy to combat the COVID-19 pandemic.

Main Text

SARS-CoV-2 was first detected in China in December 2019; within six months a variant with a D614G substitution in the viral spike protein became the predominant circulating strain globally. While the D614G variant did not evade antibody-mediated neutralization, enhanced replication and transmissibility of the variant were confirmed in multiple animal models by different groups[1-3]. Enhanced transmissibility and a larger infected population likely led to diversification of the D614G variant into many new lineages. In December 2020, the United Kingdom reported increased transmission of a novel variant of concern (VOC) 202012/01[4], also referred to as the Alpha (or B.1.1.7, Pango nomenclature) variant[5]. The Alpha variant rapidly disseminated and became the predominant circulating strain in many countries, including the United States (US)[6,7] (**Fig. 1**). Meanwhile, the Beta (i.e., B.1.351) and Gamma (i.e., P.1) variants were first detected in South Africa in May 2020 and in Brazil in November 2020, respectively, where each variant became the predominant lineage in its respective geographic region[8-10]. By August 2021, the Delta variant (B.1.617.2), which was first identified in India[11], had displaced the Alpha variant and become the predominant variant within the US (**Fig. 1**) and globally. The Omicron variant (B.1.1.529), which was first reported in late November, is rapidly spreading as of December 2021 and on pace to displace the Delta variant in many regions of the world (**Fig. 1**). The World Health Organization (WHO) and national health authorities, such as the US government SARS-CoV-2 Interagency Group (US-SIG), have designated selected SARS-CoV-2 variants as VOCs or VOIs (**Extended Data Table 1**) based on genomic analysis, transmissibility, disease severity, and, most importantly, impact on the performance of therapeutics or vaccines. Continuous monitoring

68 and rapid characterization of VOCs, VOIs, and other new variants are critical to alleviating the
69 devastating impact of the current pandemic.
70
71 As mRNA vaccines were the earliest and primary form of COVID-19 vaccines administered in the
72 US, we systematically evaluated the neutralization efficiency of U.S. mRNA vaccinee sera against
73 all VOCs and VOIs designated by the WHO Virus Evolution Working Group or US-SIG. To
74 characterize emerging variants in the shortest time frame, particularly in periods which lacked
75 clinical isolates in the US, we generated SARS-CoV-2 fluorescent reporter viruses with VOC and
76 VOI spike substitutions and deletions in the progenitor Wuhan-Hu-1 virus (designated as 614D in
77 this study) by reverse genetics (**Extended Data Table 1**). The reporter SARS-CoV-2 viruses were
78 designed to behave similarly to their clinical isolate counterparts in neutralization assays due to
79 an identical variant spike protein, which is the sole antigen of all vaccines authorized in the US.
80 The spike glycoproteins of many VOI/VOC lineages have subtle differences within the lineages,
81 and the sequence of spike protein used in our studies represent the consensus for the variant
82 lineage or represent a more divergent one from the progenitor within that lineage (**Extended Data**
83 **Table 1**). For example, the spike of Beta variant tested includes R246I in the N-terminal domain
84 (NTD), which is not found in all Beta lineage viruses.
85
86 Using a focus reduction neutralization test (FRNT), we detected minimal impact of the D614G
87 substitution (designated as virus 614G) on the neutralizing activity of the vaccinee sera (fully
88 vaccinated, 2-to-6 weeks post second dose), compared to the progenitor 614D reference virus,
89 of which the spike sequence is most closely related to what was used in mRNA vaccines (**Fig.**
90 **2a**). The Alpha variant (B.1.1.7) showed slightly decreased neutralizing antibody titers while the
91 Gamma (P.1), Delta (B.1.617.2 and AY.4.2), Epsilon (B.1.427/B.1.429), Zeta (P.2), Eta (B.1.525),
92 Iota (B.1.526/B.1.526.1), Lambda (C.37), and B.1.617.3 variants showed greater titer reductions
93 but were <4-fold reduced compared to the 614D virus. The Beta (B.1.351), Theta (P.3), Kappa
94 (B.1.617.1), Mu (B.1.621), and Omicron (B.1.1.529) variants showed ≥4-fold reductions in titers,
95 with the Omicron variants showing the greatest escape from neutralization with a 38-fold reduction
96 compared to 614D (**Fig. 2a**).
97
98 As the prevalence of variants rose within the US (**Fig. 1**), the Centers for Disease Control and
99 Prevention (CDC) received an increased number of clinical specimens from state public health
100 laboratories and other CDC collaborating laboratories through the National SARS-CoV-2 Strain
101 Surveillance (NS3) system (https://www.cdc.gov/coronavirus/2019-ncov/variants/cdc-role-

102 surveillance.html). We isolated representative variants from these clinical specimens for
103 characterization by FRNT and sequenced the stocks to ensure the spike correctly represented
104 the appropriate variant lineage. Although the reductions in neutralization differed slightly, they
105 were generally consistent between the reporter viruses and clinical isolates. Prior to the
106 emergence of Omicron, the Beta variant was the most resistant to neutralization, followed by Mu,
107 Kappa and B.1.617.3. The Gamma and Delta variants showed modest escape from
108 neutralization, and the Alpha variant neutralization was not significantly reduced as compared to
109 the 614D reference virus (**Fig. 2b**). Lambda was the only variant that showed a difference
110 between the reporter virus and the clinical isolate, which had an approximate 3-fold reduction
111 versus 1-to-1.2-fold reduction in neutralizing titers, respectively (**Fig. 2a** and **2b**). The Lambda
112 variant has at least 14 substitutions/deletions in the spike (**Extended Data Table 1**) and the
113 limited resistance to neutralization (1-to-1.2-fold) of clinical isolates was surprising. Two Lambda
114 clinical isolates (**Fig. 2b**, Lambda-S1 and -S2) with slightly different spike sequences were
115 analyzed (**Extended Data Table 1**), and the results were consistent. The reporter SARS-CoV-2
116 system is powerful because the only difference between the viruses being analyzed is the spike,
117 whereas natural isolates have many differences throughout the genome and it's possible that
118 changes in other gene products (e.g., membrane protein or envelope protein) could impact spike
119 and/or neutralization phenotype but this remains to be understood.
120
121 Shortly after the first case of Omicron was confirmed in the US on December 1, we isolated
122 multiple Omicron variants from clinical specimens. Independently, we also collected sera from US
123 vaccinees who received the third dose of a COVID-19 mRNA vaccine (booster) on the day of the
124 booster vaccination (referred as pre-booster sera) and 2-to-6 weeks after the booster vaccination
125 (referred as booster sera). The booster sera had much higher neutralizing titers against the
126 progenitor virus (614D), compared to the post-second-dose sera (**Fig. 2**) or pre-booster sera
127 (**Extended Data Fig. 1**). The booster sera had relatively high neutralizing titers against the
128 Omicron variant at levels comparable to the titers of pre-booster sera against the 614D virus
129 (**Extended Data Fig. 1**). While the post-second-dose sera and pre-booster sera had comparable
130 reductions in neutralization activities (34-to-38-fold reduction), the booster sera had neutralizing
131 activities against the Omicron variant with an average of 19-fold reduction in neutralization titers
132 (**Fig. 2a** and **Extended Data Fig. 1**). Despite the increased neutralization titers detected in
133 booster sera, the substantial reductions in neutralizing titers against Omicron viruses relative to
134 the 614D vaccine reference virus suggests potential for vaccine escape post booster as immunity
135 wanes.

Currently circulating variants are acquiring additional substitutions/deletions, which may further affect transmission, disease severity, or vaccine effectiveness and require prompt evaluation. Utilizing the short turnaround time of reverse genetics, we generated additional Alpha and Beta reporter viruses to examine the effects of specific substitutions that occurred in nature (**Fig. 2c**). While the 3 deletions and 7 substitutions in the Alpha variant spike protein (**Extended Data Table 1**) had a very small impact (1.3-fold) on neutralizing activity of vaccinee sera, we found the addition of the single E484K substitution in spike reduced the neutralizing titer of the Alpha variant by an additional 1.6-fold (2.1-fold compared to the 614D) (**Fig. 2c**). The importance of spike-E484K is further demonstrated in a Beta reporter virus that encoded the spike-484 reversion (B.1.351+K484E), which was found to be 3-fold more susceptible to neutralization compared to an unmodified Beta variant B.1.351 (2.0-fold vs 6.1-fold) (**Fig. 2c**). Interestingly, the N501Y substitution had little impact on the neutralization of the Beta variants (5.6-fold vs. 6.1-fold). A reporter virus containing substitutions only in the Beta variant receptor binding domain (RBD) (B.1.351-RBD, K417N+E484K+N501Y+D614G) was 1.7-fold more susceptible to neutralization compared to the Beta variant with full substitutions/deletions (i.e., 3.6-fold for B.1.351-RBD vs. 6.1-fold for wild type Beta). This result indicates the N-terminal domain (NTD) mutations also contribute to virus neutralization escape. This was confirmed by a Beta variant that only contains mutations in the NTD (B.1.351-NTD, L18F+D80A+D215G+L241-+L242-+A243-+R246I+614G), which reduced the neutralizing titers by 2.6-fold, compared to the 614D virus (**Fig. 2c**). Considering the plasticity of the SARS-CoV-2 spike to substitutions and deletions, as well as the recombination-prone nature of coronaviruses, substitutions and deletions present in current variants may also occur in future variants in different combinations or in different genetic backgrounds. Therefore, it is important to use reverse genetics or other focused approaches to assess the impact and understand the functionality of specific mutations in naturally occurring variants.

To better understand the effect of variant spikes on viral fitness in the presence and absence of neutralizing antibodies, we compared the replication of reporter viruses with the variant spikes in Calu-3 cells, which are a human lung epithelial cell line (**Fig. 2d**). In the absence of inhibitory sera, while Delta replicated to significantly higher titer than the original S-614D reference virus, its infectious titer was comparable to the S-614G virus and many other variants. Interestingly, in the presence of sera, even highly diluted, the titers of 614D and 614G viruses were reduced by more than 7-fold at 2x sera concentration ($FRNT_{50}$ = 2) and more than 300-fold at 5x sera concentration

170 ($FRNT_{50}$ = 5). As anticipated from neutralization escape data (**Fig. 2a**), the Beta and Omicron
171 variants replicated efficiently in the presence of both concentrations of sera (**Fig. 2d**). Intriguingly,
172 the Delta variant also replicated efficiently and only had a 3-fold reduction in titer at 5x sera
173 concentration (**Fig. 2d**). The Delta variant's ability to replicate efficiently in the presence of sub-
174 neutralizing concentrations of antisera may have facilitated infections of people with low-to-
175 modest levels of neutralizing antibodies induced by prior infection or vaccination. The immune
176 evasion of Delta variant may be an additive or synergistic result of spike mutations that reduce
177 neutralizing activity and fitness advantages (e.g., better S1/S2 cleavage and cell entry) that are
178 unrelated to neutralization but enhance replication and transmission.
179
180 Notably, all post-second-dose sera tested neutralized these variants with $FRNT_{50}$ titers higher
181 than 10 and most of them higher than 40, except against the Omicron variant, which had
182 neutralizing titers between 5 and 40 (**Fig. 2** and **Supplementary Table 1**). It has been widely
183 accepted in the influenza vaccine field that a neutralizing titer (hemagglutination inhibition titer) of
184 40 or higher is deemed protective (>50% reduction of infection rate)[12] and a 8-fold reductions in
185 neutralization *in vitro* is a consideration for updating the influenza vaccine strain. For COVID-19
186 vaccines, few studies on correlates of protection have been published but suggest a titer of 50-
187 100 is the minimum protective neutralizing titer[13,14] and the fold reduction warranting a vaccine
188 change have yet to be determined. This is also complicated by the unknown role of other effectors
189 in vaccine protection such as memory B-cell or T cell immunity[15]. However, the level of
190 neutralizing antibody titer is apparently predictive of the level of immune protection[16-19]. As
191 neutralizing antibodies wane over time[20] (**Fig. 2a** and **Extended Data Fig. 1**), infections in fully
192 vaccinated persons by variants circulating at high prevalence are likely to increase. This is
193 especially true for the Omicron variant because the number and location of changes in the S result
194 in considerable antibody escape. Nevertheless, vaccines do prevent and attenuate COVID-19[21]
195 and anamnestic responses provided through rapid expansion of memory cells should accelerate
196 viral clearance. Therefore, closely monitoring the emergence of variants resistant to neutralization
197 is a necessary and urgent task, and vaccination, including booster doses, remains the most
198 effective strategy to combat the COVID-19 pandemic.
199
200 **Acknowledgments:**
201 We acknowledge the hundreds of publications each containing neutralization results on some of
202 the VOCs or VOIs reported in this manuscript for which we regret for not being able to cite due to
203 the limitation on the number of references. We thank César G Albariño, Dennis Bagarozzi, Jessica

Chen, Jennifer Folster, Matthew Keller, Jimma Liddell, Ji Liu, Gillian McAllister, Magdalena Medrzycki, Krista Queen, Shannon Rogers, Jarad Schiffer, Maria Solano, Sarah Talarico, Brett Whitaker, Jiangwei Yao, and Natosha Zanders for coordination, testing, or analysis support. This work was funded and supported by the CDC COVID-19 Emergency Response and part of the sequencing effort was made possible through support from the CDC Advanced Molecular Detection (AMD) program. Use of trade names is for identification only and does not imply endorsement by the US Centers for Disease Control and Prevention or the US Department of Health and Human Services. The findings and conclusions in this report are those of the authors and do not necessarily represent the official position of the US Centers for Disease Control and Prevention.

Methods:

Ethics statement

Vaccinee serum samples were collected from individuals through the Influenza and Other Viruses in the Acutely Ill (IVY) Network, a Centers for Disease Control and Prevention (CDC)-funded collaboration to monitor the effectiveness of SARS-CoV-2 vaccines among US adults. Participants had no prior or current diagnosis of infection with SARS-CoV-2 and were fully vaccinated (at least 14 days after the second dose or the third dose) with either Pfizer-BioNTech mRNA vaccine BNT162b2 or Moderna mRNA-1273 vaccine (**Supplementary Table 1**). This activity was approved by each participating institution, either as a research project with written informed consent or as a public health surveillance project without written informed consent. This activity was also reviewed by the CDC and conducted in a manner consistent with applicable federal laws and CDC policies: see e.g., 45 C.F.R. part 46.102(l)(2), 21 C.F.R. part 56; 42 U.S.C. §241(d); 5 U.S.C. §552a; 44 U.S.C. §3501 et seq.

Biosafety statement

All work involving infectious SARS-CoV-2 virus, including recombinant reporter virus, was performed in CDC Biosafety Level 3 facilities with enhanced practices (BSL-3E). All personnel working with the virus were trained with relevant safety and procedure-specific protocols and their competency for performing the work in the BSL-3E laboratories was certified Recombinant DNA work was approved by CDC's Institutional Biosafety Committee (IBC). For sequencing, virus was inactivated following protocols approved by CDC's Laboratory Safety Review Board (LSRB) with a witness confirming that all steps were performed correctly to ensure complete inactivation of

237 virus. After receiving appropriate approvals, inactivated virus was transferred to BSL-2E
238 laboratories for downstream processing.
239
240 **Prevalence analysis of variants**
241 SARS-CoV-2 variant statistics for US specimens reported in the National SARS-CoV-2 Strain
242 Surveillance (NS3) and CDC-contracted networks were extracted from a distributed data
243 warehouse and rendered in Tableau Desktop (version 2021.1.1). Daily proportionalities were
244 aggregated by attributed Pangolin (version 3.1.17) lineage assignment including variants of
245 concern (VOC), variants of interest (VOI), and lineages with published World Health Organization
246 (WHO) nomenclature[5]. Pangolin sub-lineages with shared WHO aliases were consolidated:
247 B.1.1.7 and Q sub-lineages (Alpha); B.1.351, B.1.351.2, B.1.351.3 and B.1.351.5 (Beta); P.1 and
248 P.1 sub-lineages (Gamma); B.1.617.2 and AY sub-lineages (Delta); B.1.621 and B.1.621.1 (Mu);
249 and B.1.1.529 and BA sub-lineages (Omicron). Unassigned variants and Pangolin lineages
250 encoding an aspartate (D) or glycine (G) at position 614 were assigned respective "614D" and
251 "614G" labels. Variants that did not satisfy the above criteria were consolidated into "Other
252 Lineage(s)." Clinical statistics included all daily cases and deaths reported to the CDC
253 surveillance network with marked consent. Applied data analytics excluded non-contracted US
254 and global surveillance statistics to limit the impact of non-standardized reporting methodologies
255 and regional over-sampling bias within our dataset.
256
257 **Generation of SARS-CoV-2 reporter viruses**
258 **Risk-benefit analysis.** A comprehensive risk-benefit analysis was conducted for using
259 recombinant SARS-CoV-2 reporter viruses in neutralization assays. Briefly, the benefits of using
260 the reporter viruses are: 1) enabling rapid characterization of variants before they are detected in
261 the United States or before CDC receives specimens; 2) eliminating all fixation and staining steps
262 in neutralization assays, shortening the time infectious samples are handled, and reducing
263 chemical safety risks (e.g., formalin) by removing the need to fix cells; 3) minimizing the impact
264 of substitutions in non-spike genes on neutralizing titers, as changes solely reflect the effect of
265 spike mutations; 4) enabling assessment of impact of individual or specific sets of spike mutations;
266 5) enabling more consistent comparisons as isolates from different clinical specimens were noted
267 to have distinct growth properties even though they were from the same lineage. The associated
268 risk assessments are: 1) reporter viruses are different from any natural virus and created by
269 introducing the spike mutations from a new variant into the backbone virus (progenitor strain
270 Wuhan-Hu-1). The transmissibility of a particular resultant virus could be somewhere between the

271 progenitor virus and the natural variant; 2) as there is limited epidemiological or clinical evidence
272 to suggest spike mutations present in SARS-CoV-2 variants increase pathogenicity, it is most
273 likely the pathogenicity of the reporter viruses will be equivalent or reduced as compared to the
274 progenitor strain or the variant strain; 3) all naturally occurring SARS-CoV-2 variants descending
275 from the progenitor strain have acquired mutations in other genes along with the spike gene. It is
276 possible that some of the non-spike mutations may decrease the transmissibility or pathogenicity
277 of the variant, in which case a reporter virus may be more transmissible or pathogenic than the
278 variant. However, sequence analysis and literature review indicate this risk is very low, especially
279 regarding its potential public health impact during this ongoing pandemic. The safeguard and
280 mitigation strategies are: 1) the backbone of the reporter virus are based on the Wuhan-Hu-1
281 strain, which is expected to be the least transmissible strain compared to later variants; 2) a
282 mNeonGreen reporter gene replaces the ORF7a in the reporter virus, which may attenuate the
283 virus as the ORF7a protein has been reported to be an interferon antagonist[22,23]; 3) mutations
284 engineered into a reporter virus are either part of or all of the spike mutations found in a natural
285 isolate and the engineering of unnatural mutations is prohibited; 4) the reporter viruses are only
286 to be used in *in vitro* studies, such as neutralization assays, and not in *in vivo* studies; 5) all the
287 *in vitro* work is conducted in BSL-3E facilities including enhanced practices such as shower out
288 after experiments to minimize the possibility of accidental release of the reporter virus to the
289 environment; 6) all staff working with the reporter viruses are fully vaccinated; 7) all staff are
290 approved for working with BSL-3E select agents with senior staff having decades of BSL-3E
291 experience working with highly pathogenic viruses. The **conclusion** is: under the current public
292 health emergency, with the urgency for antigenic surveillance of variants, the benefits of using
293 SARS-CoV-2 reporter viruses exceeds the risks associated with generating and using
294 recombinant reporter viruses. These risks are believed to be extremely low after mitigation.
295
296 **DNA construct.** The DNA constructs were either generated as linear fragments as previously
297 described[24] or generated as a cloned DNA as detailed here. The DNA clone for SARS-CoV-2
298 strain Wuhan-Hu-1 (GenBank accession number: NC_045512) was purchased from Codex DNA
299 (San Diego, CA). The viral genome was flanked by a T7 promoter sequence at the 5' end and a
300 linearization site at the 3' end. The whole cassette was cloned into a bacterial artificial
301 chromosome (BAC) vector. The DNA clone was modified to replace the ORF7a gene with a
302 human codon-optimized mNeonGreen gene (GenBank accession number: AGG56535.1)
303 following the same design as reported previously[24]. The spike gene of this progenitor reporter
304 virus was excised by AscI and BamHI-HF restriction enzymes, resulting in a linearized vector into

305 which synthetic variant spike genes can be assembled using Gibson Assembly (NEB). The
306 Gibson Assembly reaction was then transformed into TransforMax™ EPI300™ Electrocompetent
307 *E. coli* (Lucigen). Transformations were immediately recovered in SOC medium at 30℃ for 1
308 hour, and plated on LB agar plates containing 25 µg/ml chloramphenicol, followed by
309 approximately 2 days of incubation at 30℃. Colonies were picked and inoculated into LB broth
310 containing 25 µg/ml chloramphenicol for approximately 16±2 hours followed by induction for
311 approximately 4±1 hours at 30℃. DNA was extracted and the sequence was verified by Illumina
312 next-generation sequencing (NGS).
313
314 ***In vitro* transcription**. Infectious clones were linearized by SbfI-HF digestion and cleaned up by
315 phenol:chloroform:isoamyl alcohol (PCIA) (25:24:1) extraction. Full-length viral RNA was
316 generated using the T7 RiboMAX™ Express Large Scale RNA Production System with slight
317 modifications to manufacturer's instructions (Promega). Briefly, reaction components were
318 adjusted such that in a 50 µL reaction the final concentration of ATP, CTP, and UTP was 7.5 mM,
319 GTP was 3.5 mM, and the Anti-Reverse Cap Analog (NEB) was used at 2.8 mM. After 2-3 hours
320 of incubation at 30℃, RNA was cleaned up by PCIA and ethanol precipitated for at least 1 hour.
321 Quality of the RNA was assessed by UV-vis spectroscopy and denaturing agarose gel
322 electrophoresis.
323
324 **Nucleocapsid protein expressing cell line.** Vero E6 cells (ATCC, CRL-1586) were transfected
325 using Lipofectamine 3000 (Invitrogen) with a plasmid encoding SARS-CoV-2 nucleocapsid
326 protein via CMV3 promoter as well as mCherry2 via an IRES element. Transfected cells were
327 placed under drug selection (0.1-0.3 mg/ml geneticin) to establish the pooled bulk population.
328 Stable single-cell clones were selected from the bulk population by serial dilution plating and drug
329 selection. The expression of nucleocapsid protein was confirmed by the SARS-CoV-2
330 Nucleocapsid Protein ELISA Kit (ABclonal, Woburn, MA) and the cell clone supporting the most
331 efficient virus rescue was selected (VeroE6-N). Cells were maintained in DMEM supplemented
332 with 10% FBS and 0.2 mg/ml geneticin.
333
334 **Virus rescue.** To rescue the SARS-CoV-2 reporter virus, VeroE6-N cells were trypsinized,
335 washed with Opti-MEM (ThermoFisher) and resuspended in 100 µL nucleofector solution at a
336 concentration of 1.5 x 10^6 cells/100 µl following the instructions of the Nucleofector Kit V (Lonza).
337 *In vitro* transcribed RNA (5 µg) was added to the cells and the cell-RNA mixture was transferred
338 into an electroporation cuvette. Electroporation was completed using the Program T-024 of the

339 Nucleofector 2b device (Lonza). Electroporated cells were immediately transferred into a 6-well
340 plate pre-filled with 2 ml/well of pre-warmed Opti-MEM. At 18-24 hours post-transfection,
341 supernatant was collected (P0) and inoculated onto a monolayer of VeroE6/TMPRSS2 cells[25]
342 (JCRB1819, JCRB Cell Bank). Twenty-four hours post-inoculation, supernatant was collected to
343 make the seed stock (P1). P1 was propagated in T-150 flasks of VeroE6/TMPRSS2 cells at a
344 multiplicity of infection (MOI) of 0.02-0.1 for 24 hours to make the P2 working stock. The working
345 stock was sequenced as described below.
346
347 **Sequence confirmation.** All the SARS-CoV-2 reporter viruses were sequenced by NGS to
348 confirm the sequence of the spike gene. Total RNA was extracted from the working stock of each
349 reporter virus and treated with DNase using the DNase Max kit (Qiagen) following manufacturer's
350 instructions. Five microliters of resulting clean RNA was used for first- and second-strand cDNA
351 synthesis and library preparation using NEB Ultra II Directional RNA library prep kit for Illumina
352 (New England Biolabs, Ipswich, MA, USA). Libraries were barcoded with unique dual indices
353 synthesized in the CDC Biotechnology Core Facility Oligonucleotide Synthesis Laboratory.
354 Resulting libraries were analyzed for size using the Agilent Fragment Analyzer (Agilent
355 Technologies, Inc., Santa Clara, CA) and quantified using the Qubit 4 Fluorometer (Thermo
356 Fischer Scientific, Waltham, MA). Libraries were normalized to equimolar concentrations, pooled,
357 and sequenced on Illumina NovaSeq 6000 (Illumina, San Diego, CA, USA) using the NovaSeq
358 v1.5 SP Reagent Kit (300 cycles). Demultiplexed reads were processed and assembled using the
359 Iterative Refinement Meta-Assembler (IRMA) on a custom CoV-recombinant configuration[26]. The
360 614D reporter virus (Wuhan-Hu-1 strain with the ORF7a gene replaced by mNeonGreen) was
361 used as the reference. Reads were filtered for a minimum median phred score (Q score) of 27
362 and a minimum read length of 80 bases. A Striped Smith-Waterman algorithm was selected for
363 read alignment, and final assembly was performed against the reference sequence matched
364 during read gathering. Amended consensus genomes were created from plurality
365 assemblies by ambiguation of bases with coverage < 20x to 'N', and positions with a minor allele
366 frequency (MAF) > 0.2 were given ambiguous nucleotide codes according to IUPAC conventions.
367 Quality metrics were calculated using a count of non-ambiguated amended consensus bases to
368 show proportion of recombinant genome assembled, and average coverage depth across the
369 genome was noted. The full genome sequences of all the viruses are being deposited in GenBank
370 and accession numbers will be provided.
371
372 **MSD binding assays**

373 Serum samples were analyzed at 1:100 and 1:5000 dilutions for IgG, IgM, and IgA to SARS-
374 CoV-2 nucleocapsid (N), SARS-CoV-2 S1 receptor binding domain (RBD), and SARS-CoV-2
375 spike (S) protein (V-PLEX SARS-CoV-2 Panel 2 Kit, Meso Scale Discovery, Rockville, MD), as
376 described previously[27]. Serum antibody levels were calculated using Reference Standard 1 and
377 converted to WHO International Binding Antibody Units (BAU/mL) per manufacturer kit
378 instructions.
379
380 **Focus Reduction Neutralization Test (FRNT)**
381 **Reporter virus-based assay.** Serum specimens were heat-inactivated at 56℃ for 30 minutes,
382 aliquoted, and stored at -80℃. Each serum sample was serially diluted in 3-fold steps (1:40–
383 1:29,160) in sextuplicate in 96-well round bottom plates. SARS-CoV-2 reporter virus was diluted
384 to 3,200-4,000 focus forming units (FFUs) per ml. Diluted serum samples were mixed with an
385 equal volume of diluted virus and incubated for 1 hour at room temperature (21±2℃). Media from
386 confluent monolayer VeroE6/TMPRSS2 in 96-well tissue culture plates was removed, and 50 µl
387 of the serum–virus mixture was inoculated into each well of cells and incubated at 37℃ in a 5%
388 CO_2 atmosphere for 2 hours. The wells were overlaid with 100 µl of 0.75% methylcellulose in
389 DMEM (Gibco), supplemented with 2% HI-FBS and 1x Pen-Strep and incubated at 33℃ in a 5%
390 CO_2 incubator for 16-18 hours. Plates were scanned using a CellInsight CX5 High-Content
391 Screening Platform (Thermo Scientific) running an 'Acquisition Only' protocol within Cellomics
392 Scan Version 6.6.0 (Thermo Scientific, Build 8153). All plates were imaged under equal exposure
393 conditions per channel and under 4x magnification.
394 Foci were identified and quantified using appropriate 'Spot Detection' protocol within Cellomics
395 Scan Version 6.6.2 (Thermo Scientific, Build 8533). Spot counts for each channel were exported
396 for further analysis in R (Version 4.0.3). $FRNT_{50}$ values were calculated by fitting the three-
397 parameter log-logistic function (LL.3) to the FFU counts paired with corresponding dilution
398 information. In cases where the Hill Constant was fit at less than 0.5, e.g., incomplete
399 neutralization, $FRNT_{50}$ values were estimated with a two-parameter fit while fixing the Hill
400 Constant to 1. The R script has been deposited in GitHub: https://github.com/CDCgov/SARS-
401 CoV-2_FRNTcalculations/.
402
403 **Clinical isolate-based assay.** SARS-CoV-2 isolates were propagated on Vero/TMPRSS2 cells.
404 All stocks were inoculated at multiplicity of infection (MOI) of approximately 0.004 or 0.01 (for
405 Omicron viruses) and harvested at 2 days post-inoculation. The viral spike sequences were
406 verified using unbiased NGS sequencing (KAPA HyperPrep library kit with RiboErase, followed

407 by Illumina sequencing). All cells and virus stocks tested negative for mycoplasma using
408 MycoAlert Plus reagents (Lonza). Heat-inactivated serum samples were serially diluted in 3-fold
409 steps in DMEM supplemented with 2% heat-inactivated fetal bovine serum (HI-FBS), 1x Pen-
410 Strep and sodium pyruvate (Gibco). The serum dilutions were mixed with an equal volume of virus
411 in the same medium (final serum dilutions 1:10-1:7,290) and incubated for 1 hour at 37℃.
412 Vero/TMPRSS2 cells growing in 96-well imaging plates were then inoculated in triplicate with 40
413 µL of serum-virus mixtures and incubated for 1 hour at 37℃ with periodic shaking of the plates.
414 Inocula were removed and cells overlaid with 1.5% medium viscosity carboxymethylcellulose
415 (Sigma-Aldrich) in MEM (Gibco), supplemented with 4% HI-FBS, 1x Penicillin-Streptomycin
416 (pen/strep), and sodium pyruvate. Twenty hours later, the overlay was washed off with PBS, and
417 cells fixed with 10% neutral-buffered formalin, permeabilized with 0.5% Triton X100 in PBS,
418 blocked with 1% bovine serum albumin in PBS, and stained using SARS/SARS-CoV-2
419 Coronavirus Nucleocapsid Monoclonal Antibody (Invitrogen MA5-29981) as the primary antibody
420 followed by Alexa647-conjugated secondary antibody (Invitrogen). The monolayers were imaged
421 using a BioTek Cytation3 instrument and virus foci (approximately 100-200/well in no-serum
422 control wells) were counted using Gen5 software. The foci counts were normalized to no-serum
423 controls, and 4 parameter nonlinear regression analysis with bottom constraint set to 0, and top
424 value set to 1 (GraphPad Prism v7.04) was used to fit a curve to the data and to determine the
425 FRNT50 value.
426
427 **Data processing and statistical analysis.** Geometric mean titers (GMTs) of each virus were
428 calculated using the $FRNT_{50}$ neutralizing titers of all the serum samples tested against that virus.
429 Average fold change of a variant against the 614D virus (Wuhan-Hu-1 or WA-1) was calculated
430 as the arithmetic mean of the corresponding $FRNT_{50}$ ratios (614D/variant) of each serum sample.
431 SARS-CoV-2 variants isolated from clinical specimens were tested upon availability in parallel
432 with WA-1. All serum/variant combinations were tested twice in independent experiments. In
433 Figure 2B, the arithmetic mean WA-1 $FRNT_{50}$ value for each serum is presented (2-8 independent
434 runs). For other variants, the $FRNT_{50}$ fold-differences to WA-1 were determined from two
435 independent runs per serum sample, and the $FRNT_{50}$ value resulting from this fold average and
436 the grand average $FRNT_{50}$ for WA-1 are depicted. For statistical analysis, normality test and
437 residual diagnostics were performed on the data as the assumption of normality was violated, the
438 data were analyzed using a nonparametric test in the SAS NPAR1WAY procedure. The Dwass,
439 Steel, Critchlow-Fligner method[28-30] was used for multiple comparisons. Statistical analyses were
440 performed using SAS 9.2 (SAS Institute), with p-value < 0.05 considered significant.

441

442 **Virus replication in Calu-3 cells.**

443 Calu-3 cells (Human lung epithelial cell line) were obtained from CDC's Division of Scientific
444 Resources (DSR). Cells were seeded in 12-well plates and cultured 4 to 5 days until cell
445 confluence reached 80-90% before infection. Culture media was removed from the cells before
446 infection and 200-400 focus forming unit (FFU) virus was added into each well (triplicate wells
447 for each virus). The plates were incubated at 37℃ in a 5% CO2 atmosphere for 1 hour. Ten
448 individual vaccinee serum samples from persons received Pfizer-BioNTech mRNA vaccine
449 BNT162b2 and 10 vaccinee serum samples from persons received Moderna mRNA-1273 vaccine
450 were each normalized to 500 FRNT50 (against 614D reference virus) and pooled separately
451 (500X stock). Pooled Moderna or Pfizer sera was diluted to 2X or 5X concentration (FRNT50=2
452 or 5 against 614D reference virus) in infection media (DMEM supplemented with 2% HI-FBS and
453 1x pen/strep). The inoculum was removed from each well after incubation and 1ml of infection
454 media with or without the diluted sera was added to corresponding wells (0X, 2X, or 5X FRNT50)
455 and the plates were returned to the 37℃, 5% CO2 incubator for further incubation. Two days
456 later, the culture supernatant was collected and titrated by FFU assay. The FFU assay was
457 performed similarly to the FRNT assay by serial dilution of the virus and without mixing the virus
458 with any sera. The foci acquisition and quantification steps were same as described in the FRNT
459 assay. For each variant, the viral titers in the presence of sera were compared to those in the
460 absence of sera to calculate the fold of change (reduction) in titers. The significance of the
461 reduction was analyzed by one-way ANOVA with Dunnett's multiple comparisons test (no sera
462 vs. 2X sera; no sera vs. 5X sera).

463

References:

1 Hou, Y. J. *et al.* SARS-CoV-2 D614G variant exhibits efficient replication ex vivo and transmission in vivo. *Science* **370**, 1464-1468, doi:10.1126/science.abe8499 (2020).

2 Plante, J. A. *et al.* Spike mutation D614G alters SARS-CoV-2 fitness. *Nature* **592**, 116-121, doi:10.1038/s41586-020-2895-3 (2021).

3 Zhou, B. *et al.* SARS-CoV-2 spike D614G change enhances replication and transmission. *Nature* **592**, 122-127, doi:10.1038/s41586-021-03361-1 (2021).

4 Public Health England. Investigation of novel SARS-CoV-2 variant: variant of concern 202012/01, technical briefing 3. *London, United Kingdom: Public Health England*, doi:https://assets.publishing.service.gov.uk/government/uploads/system/uploads/attachment_data/file/950823/Variant_of_Concern_VOC_202012_01_Technical_Briefing_3_-_England.pdf (2020).

5 Konings, F. *et al.* SARS-CoV-2 Variants of Interest and Concern naming scheme conducive for global discourse. *Nature Microbiology* **6**, 821-823, doi:10.1038/s41564-021-00932-w (2021).

6 Galloway, S. E. *et al.* Emergence of SARS-CoV-2 B.1.1.7 Lineage - United States, December 29, 2020-January 12, 2021. *MMWR Morb Mortal Wkly Rep* **70**, 95-99, doi:10.15585/mmwr.mm7003e2 (2021).

7 Paul, P. *et al.* Genomic Surveillance for SARS-CoV-2 Variants Circulating in the United States, December 2020-May 2021. *MMWR Morb Mortal Wkly Rep* **70**, 846-850, doi:10.15585/mmwr.mm7023a3 (2021).

8 Tegally, H. *et al.* Detection of a SARS-CoV-2 variant of concern in South Africa. *Nature* **592**, 438-443, doi:10.1038/s41586-021-03402-9 (2021).

9 Castro, M. C. *et al.* Spatiotemporal pattern of COVID-19 spread in Brazil. *Science* **372**, 821-826, doi:10.1126/science.abh1558 (2021).

10 Naveca, F. G. *et al.* COVID-19 in Amazonas, Brazil, was driven by the persistence of endemic lineages and P.1 emergence. *Nature Medicine* **27**, 1230-1238, doi:10.1038/s41591-021-01378-7 (2021).

11 Cherian, S. *et al.* SARS-CoV-2 Spike Mutations, L452R, T478K, E484Q and P681R, in the Second Wave of COVID-19 in Maharashtra, India. *Microorganisms* **9**, doi:10.3390/microorganisms9071542 (2021).

12 Hannoun, C., Megas, F. & Piercy, J. Immunogenicity and protective efficacy of influenza vaccination. *Virus Res* **103**, 133-138, doi:10.1016/j.virusres.2004.02.025 (2004).

13 Feng, S. *et al.* Correlates of protection against symptomatic and asymptomatic SARS-CoV-2 infection. *Nat Med* **27**, 2032-2040, doi:10.1038/s41591-021-01540-1 (2021).

14 McMahan, K. *et al.* Correlates of protection against SARS-CoV-2 in rhesus macaques. *Nature* **590**, 630-634, doi:10.1038/s41586-020-03041-6 (2021).

15 Sette, A. & Crotty, S. Adaptive immunity to SARS-CoV-2 and COVID-19. *Cell* **184**, 861-880, doi:10.1016/j.cell.2021.01.007 (2021).

16 Cromer, D. *et al.* Neutralising antibody titres as predictors of protection against SARS-CoV-2 variants and the impact of boosting: a meta-analysis. *The Lancet Microbe* **3**, e52-e61, doi:10.1016/S2666-5247(21)00267-6 (2022).

17 Corbett, K. S. *et al.* Immune correlates of protection by mRNA-1273 vaccine against SARS-CoV-2 in nonhuman primates. *Science* **373**, eabj0299, doi:10.1126/science.abj0299 (2021).

18 Earle, K. A. *et al.* Evidence for antibody as a protective correlate for COVID-19 vaccines. *Vaccine* **39**, 4423-4428, doi:https://doi.org/10.1016/j.vaccine.2021.05.063 (2021).

509 19 Khoury, D. S. *et al.* Neutralizing antibody levels are highly predictive of immune protection from
510 symptomatic SARS-CoV-2 infection. *Nature Medicine* **27**, 1205-1211, doi:10.1038/s41591-021-
511 01377-8 (2021).
512 20 Pegu, A. *et al.* Durability of mRNA-1273 vaccine-induced antibodies against SARS-CoV-2 variants.
513 *Science* **373**, 1372-1377, doi:10.1126/science.abj4176 (2021).
514 21 Thompson, M. G. *et al.* Prevention and Attenuation of Covid-19 with the BNT162b2 and mRNA-
515 1273 Vaccines. *New England Journal of Medicine* **385**, 320-329, doi:10.1056/NEJMoa2107058
516 (2021).
517 22 Cao, Z. *et al.* Ubiquitination of SARS-CoV-2 ORF7a promotes antagonism of interferon response.
518 *Cell Mol Immunol* **18**, 746-748, doi:10.1038/s41423-020-00603-6 (2021).
519 23 Nemudryi, A. *et al.* SARS-CoV-2 genomic surveillance identifies naturally occurring truncation of
520 ORF7a that limits immune suppression. *Cell Rep* **35**, 109197, doi:10.1016/j.celrep.2021.109197
521 (2021).
522 24 Xie, X. *et al.* An Infectious cDNA Clone of SARS-CoV-2. *Cell Host Microbe* **27**, 841-848.e843,
523 doi:10.1016/j.chom.2020.04.004 (2020).
524 25 Matsuyama, S. *et al.* Enhanced isolation of SARS-CoV-2 by TMPRSS2-expressing cells. *Proc Natl*
525 *Acad Sci U S A* **117**, 7001-7003, doi:10.1073/pnas.2002589117 (2020).
526 26 Shepard, S. S. *et al.* Viral deep sequencing needs an adaptive approach: IRMA, the iterative
527 refinement meta-assembler. *BMC Genomics* **17**, 708, doi:10.1186/s12864-016-3030-6 (2016).
528 27 Edara, V. V. *et al.* Infection- and vaccine-induced antibody binding and neutralization of the
529 B.1.351 SARS-CoV-2 variant. *Cell Host Microbe* **29**, 516-521.e513,
530 doi:10.1016/j.chom.2021.03.009 (2021).
531 28 Dwass, M. in *Contributions to Probability and Statistics* (ed I. Olkin) 198-202 (Stanford University
532 Press, 1960).
533 29 Steel, R. G. D. A Rank Sum Test for Comparing All Pairs of Treatments. *Technometrics* **2**, 197-207,
534 doi:10.2307/1266545 (1960).
535 30 Douglas, C. E. & Michael, F. A. On distribution-free multiple comparisons in the one-way analysis
536 of variance. *Communications in Statistics - Theory and Methods* **20**, 127-139,
537 doi:10.1080/03610929108830487 (1991).

538

539 **Figure Legends:**

540 **Fig. 1. Prevalence of SARS-CoV-2 variants in the United States.** SARS-CoV-2 variant
541 prevalence is shown for clinical specimens processed within the National SARS-CoV-2 Strain
542 Surveillance (NS3) and CDC-contracted networks by relative, daily incidence (dot icons) for key
543 Pangolin lineages (WHO nomenclature in parentheses), VOIs/VOCs, and specimens encoding
544 critical sequence markers (614D/G) but not belonging to those variants. Daily reported clinical
545 cases are summarized in the bar graph (right-side, Y-axis). Cut-off date is December 12, 2021.

546

547 **Fig. 2. Neutralization and inhibition of mRNA vaccinee sera against live SARS-CoV-2**
548 **viruses.** Each dot represents the neutralizing titer ($FRNT_{50}$) of an individual serum sample; at
549 least 20 post-second-dose sera were tested against each variant. The average fold changes
550 relative to reference virus 614D (set as 1-fold) are shown on the top of the graph. For each variant,
551 the average fold change is the geometric mean of the individual $FRNT_{50}$ ratios (614D/variant)
552 calculated for each serum sample. Dashed line represents the limit of quantitation (LOQ). **(a)** All
553 WHO and US-SIG designated SARS-CoV-2 variants of concern (VOCs) and variants of interest
554 (VOIs) were tested using reporter viruses. The geometric mean $FRNT_{50}$ titers are shown on the
555 graph with standard deviation. LOQ(o)=5 for Omicron and LOQ=40 for all other variants. The
556 average fold changes of all variants differ significantly (P<0.0001) from 614D, except for 614G
557 (P=0.9999). **(b)** VOCs and selected VOIs isolated from clinical specimens were tested. The
558 average fold change of all variants differs significantly (P<0.001) from 614D, except for B.1.1.7
559 (P=0.9995) and the two C.37 viruses (C.37(λ) S1 and S2). **(c)** Reporter viruses with or without
560 specific substitutions were tested to illustrate the impact of specific substitutions. B.1.351 + Y501N
561 has the reversion to original N at 501 of S, and B.1.351 + K484E has a reversion to original E at
562 484 of S. B.1.351-RBD contains the K417N, E484K, N501Y substitutions in RBD along with the
563 downstream D614G substitution. B.1.351-NTD contains the mutations in NTD along with the
564 downstream D614G. Thin gray lines link the same serum sample tested against the different
565 viruses. The thick black line links the geometric mean titers of different variants. **(d)** Calu-3 cells
566 were infected with 200-400 focus forming unit (FFU) of each virus and incubated for 2 days in
567 media with or without sera. The sera were pooled from the individual sera used in (a) and diluted
568 to 2X or 5X concentration (diluted sera titer FRNT50 = 2 or 5 against 614D reference virus). The
569 viruses were collected from Calu-3 supernatant at 2 days post inoculation and titrated by FFU
570 assay. Titer differences are marked as *, representing p<0.05 (One-way ANOVA) for statistical
571 significance, compared to the no sera control within each variant group. Fold changes (reductions)
572 compared to the no sera control are shown on the top of the panel.

573 **Extended Data Fig. 1. Neutralization activity against live SARS-CoV-2 viruses of mRNA**
574 **vaccine sera collected pre- and post-booster vaccination.** Pre-booster sera were collected
575 on the day of booster vaccination and post-booster sera were collected 2-to-6 weeks post booster
576 vaccination. Viruses were isolated from clinical specimens. The average fold changes relative to
577 reference virus 614D (set as 1-fold for pre-booster and post-booster, respectively) are shown on
578 the top of the graph. For each variant, the average fold change is the geometric mean of the
579 individual FRNT50 ratios (614D/variant) calculated for each serum sample. Dashed line
580 represents the limit of quantitation (LOQ). For samples with titer below LOQ the values are still
581 shown and used in calculating the fold change, but they should be interpreted as qualitative
582 instead of quantitative.
583
584 **Extended Data Table 1. List of sequence-confirmed substitutions and deletions present in**
585 **the spike protein of the viruses used in this study.**
586
587 **Supplementary Table 1. Quantification post-second-dose sera for nucleocapsid, spike and**
588 **RBD binding antibody units as well as neutralizing antibody titers against 614D and Delta**
589 **variant (B.1.617.2).**
590

Figure 1

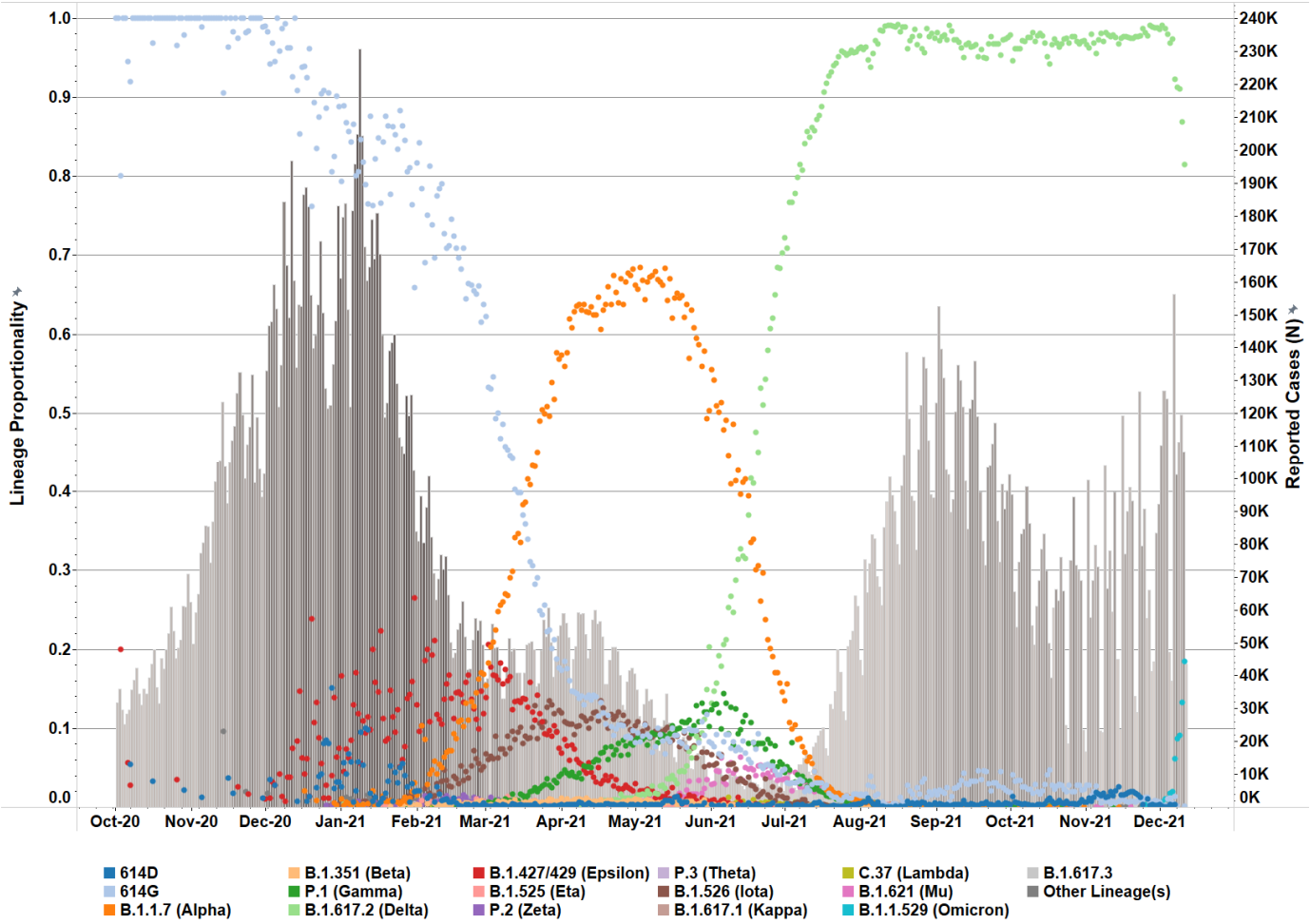

Fig. 1. Prevalence of SARS-CoV-2 variants in the United States. SARS-CoV-2 variant prevalence is highlighted for clinical specimens processed within US National SARS-CoV-2 Strain Surveillance networks by relative, daily incidence (dot icons, 0.0 to 1.0) for key Pangolin lineages (WHO nomenclature in parentheses), VOI/VOCs, and specimens encoding critical sequence markers (614D/G) but do not belong to those variants. Daily, reported clinical cases are summarized in the bar graph (right-side, dual Y-axis). Cut-off date is December 12, 2021.

Figure 2

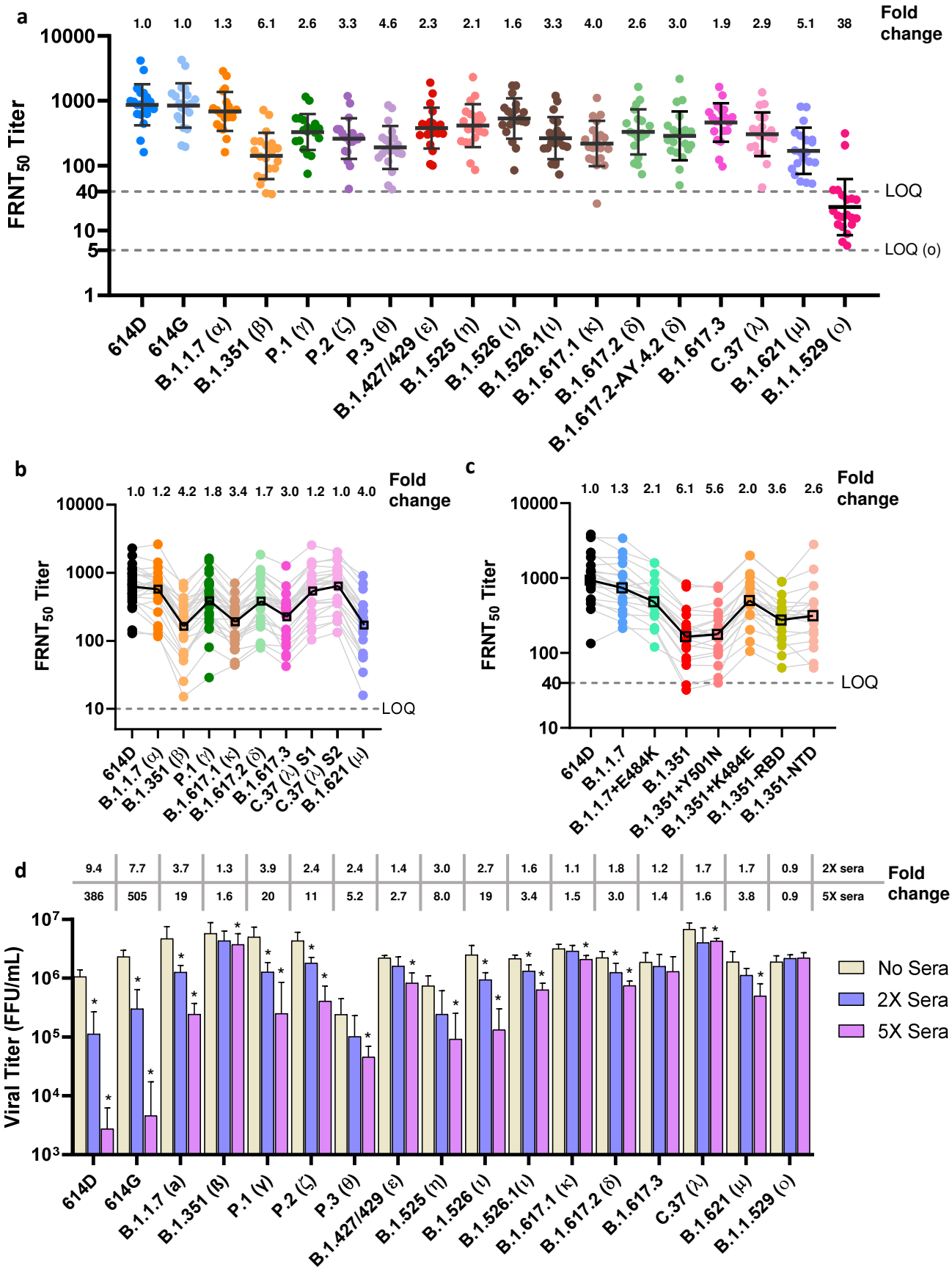
a
Fold change
1.0 1.0 1.3 6.1 2.6 3.3 4.6 2.3 2.1 1.6 3.3 4.0 2.6 3.0 1.9 2.9 5.1 38
FRNT50 Titer
10000
1000
100
40
10
5
1
LOQ
LOQ (o)
614D
614G
B.1.1.7 (α)
B.1.351 (β)
P.1 (γ)
P.2 (ζ)
P.3 (θ)
B.1.427/429 (ε)
B.1.525 (η)
B.1.526 (ι)
B.1.526.1(ι)
B.1.617.1 (κ)
B.1.617.2 (δ)
B.1.617.2-AY.4.2 (δ)
B.1.617.3
C.37 (λ)
B.1.621 (μ)
B.1.1.529 (ο)
b
Fold change
1.0 1.2 4.2 1.8 3.4 1.7 3.0 1.2 1.0 4.0
FRNT50 Titer
10000
1000
100
10
LOQ
614D
B.1.1.7 (α)
B.1.351 (β)
P.1 (γ)
B.1.617.1 (κ)
B.1.617.2 (δ)
B.1.617.3
C.37 (λ) S1
C.37 (λ) S2
B.1.621 (μ)
c
Fold change
1.0 1.3 2.1 6.1 5.6 2.0 3.6 2.6
FRNT50 Titer
10000
1000
100
40
10
LOQ
614D
B.1.1.7
B.1.1.7+E484K
B.1.351
B.1.351+Y501N
B.1.351+K484E
B.1.351-RBD
B.1.351-NTD
d
Fold change
2X sera: 9.4 7.7 3.7 1.3 3.9 2.4 2.4 1.4 3.0 2.7 1.6 1.1 1.8 1.2 1.7 1.7 0.9
5X sera: 386 505 19 1.6 20 11 5.2 2.7 8.0 19 3.4 1.5 3.0 1.4 1.6 3.8 0.9
Viral Titer (FFU/mL)
10^7
10^6
10^5
10^4
10^3
No Sera
2X Sera
5X Sera
614D
614G
B.1.1.7 (α)
B.1.351 (β)
P.1 (γ)
P.2 (ζ)
P.3 (θ)
B.1.427/429 (ε)
B.1.525 (η)
B.1.526 (ι)
B.1.526.1(ι)
B.1.617.1 (κ)
B.1.617.2 (δ)
B.1.617.3
C.37 (λ)
B.1.621 (μ)
B.1.1.529 (ο)

Fig. 2. Neutralization and inhibition of mRNA vaccinee sera against live SARS-CoV-2 viruses. Each dot represents the neutralizing titer ($FRNT_{50}$) of an individual serum sample; at least 20 post-second-dose sera were tested against each variant. The average fold changes relative to reference virus 614D (set as 1-fold) are shown on the top of the graph. For each variant, the average fold change is the geometric mean of the individual $FRNT_{50}$ ratios (614D/variant) calculated for each serum sample. Dashed line represents the limit of quantitation (LOQ). **(a)** All WHO and US-SIG designated SARS-CoV-2 variants of concern (VOCs) and variants of interest (VOIs) were tested using reporter viruses. The geometric mean $FRNT_{50}$ titers are shown on the graph with standard deviation. LOD=5 for Omicron and LOD=40 for all other variants. The average fold changes of all variants differ significantly ($P<0.0001$) from 614D, except for 614G ($P=0.9999$). **(b)** VOCs and selected VOIs isolated from clinical specimens were tested. The average fold change of all variants differs significantly ($P<0.001$) from 614D, except for B.1.1.7 ($P=0.9995$) and the two C.37 viruses (C.37(λ) S1 and S2). **(c)** Reporter viruses with or without specific substitutions were tested to illustrate the impact of specific substitutions. B.1.351 + Y501N has the reversion to original N at 501 of S, and B.1.351 + K484E has a reversion to original E at 484 of S. B.1.351-RBD contains the K417N, E484K, N501Y substitutions in RBD along with the downstream D614G substitution. B.1.351-NTD contains the mutations in NTD along with the downstream D614G. Thin gray lines link the same serum sample tested against the different viruses. The thick black line links the geometric mean titers of different variants. **(d)** Calu-3 cells were infected with 200-400 focus forming unit (FFU) of each virus and incubated for 2 days in media with or without sera. The sera were pooled from the individual sera used in (a) and diluted to 2X or 5X concentration (diluted sera titer FRNT50 = 2 or 5 against 614D reference virus). The viruses were collected from Calu-3 supernatant at 2 days post inoculation and titrated by FFU assay. Titer differences are marked as *, representing $p<0.05$ (One-way ANOVA) for statistical significance, compared to the no sera control within each virus group. Fold changes (reductions) compared to the no sera control are shown on the top of the panel.

Extended Data Figure 1

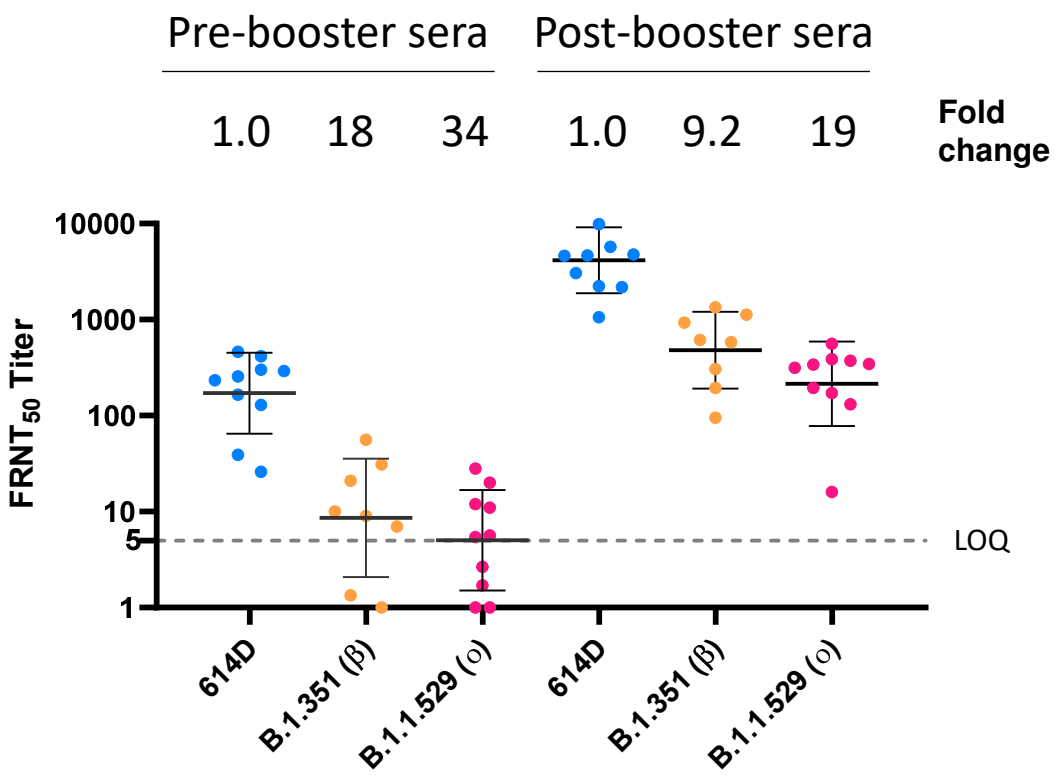

Extended Data Fig. 1. Neutralization activity against live SARS-CoV-2 viruses of mRNA vaccine sera collected pre- and post-booster vaccination. Pre-booster sera were collected on the day of booster vaccination and post-booster sera were collected 2-to-6 weeks post booster vaccination. Viruses were isolated from clinical specimens. The average fold changes relative to reference virus 614D (set as 1-fold for pre-booster and post-booster, respectively) are shown on the top of the graph. For each variant, the average fold change is the geometric mean of the individual FRNT50 ratios (614D/variant) calculated for each serum sample. Dashed line represents the limit of quantitation (LOQ). For samples with titer below LOQ the values are still shown and used in calculating the fold change, but they should be interpreted as qualitative instead of quantitative.